Molecular Endocrinology. First published January 12, 2006 as doi:10.1210/me.2004-0075

p38 MAPK Stimulates Estrogen-Mediated Transcription and Proliferation Through the Phosphorylation and Potentiation of the p160 Coactivator GRIP1

Abbreviated title: p38 MAPK Potentiates GRIP1

Daniel E. Frigo[1, 2, *], Aninda Basu[3], Erica N. Nierth-Simpson[1,2], Christopher B. Weldon[4], Christine M. Dugan[5,6], Steven Elliott[5,6], Bridgette M. Collins-Burow[5,6], Virgilio A. Salvo[5,6], Yun Zhu[5,6], Lilia I. Melnik[2], Gabriela N. Lopez[7], Peter J. Kushner[7,8], Tyler J. Curiel[5], Brian G. Rowan[3], John A. McLachlan[2,9], and Matthew E. Burow[2,4-6,**]

[1]Molecular and Cellular Biology Program, [2]Center for Bioenvironmental Research, [4]Department of Surgery, [5]Department of Medicine-Section of Hematology and Medical Oncology, [6]Tulane Cancer Center, and the [9]Department of Pharmacology, Tulane University Health Science Center, New Orleans, LA 70112, the [7]Metabolic Research Unit, [8]Department of Medicine, University of California, San Francisco, California 94143, and the [3]Department of Biochemistry and Molecular Biology, Medical College of Ohio, Toledo, OH 43614

[*]Current address: Duke University Medical Center, Department of Pharmacology and Cancer Biology, Box 3813, Durham, NC 27710

[**]Address all correspondence and requests for reprints to: Matthew E. Burow, Tulane University School of Medicine, Department of Medicine-Section of Hematology and

Medical Oncology, 1430 Tulane Ave. SL-78, New Orleans, LA 70112. Phone: (504) 988-6688; Fax: (504) 588-5483; E-mail: mburow@tulane.edu.

Key Words: ER, DDT, HEK 293, Ishikawa, MAPK, MCF-7, p38, GRIP1

This work was supported by Department of Energy Grant DE-FC26-00NT40843 (to J.A.M.), Office of Naval Research Grant N00014-99-1-0763 (to J.A.M. and M.E.B.), Center for Disease Control Grant RO6/CCR419466-02 (to J.A.M.), National Institutes of Health Grant DK059389 (to M.E.B.), and the Cancer Association of Greater New Orleans (to D.E.F.).

Abstract

Nuclear hormone receptors, such as the estrogen receptors (ERs), are regulated by specific kinase signaling pathways. Here, we demonstrate that the p38 MAPK stimulates both ERα– and ERβ-mediated transcription in MCF-7 breast carcinoma, Ishikawa endometrial adenocarcinoma, and human embryonic kidney 293 cells. Inhibition of this potentiation using the p38 inhibitor, RWJ67657, blocked estrogen-mediated transcription and proliferation. Activated ERs promote gene expression in part through the recruitment of the p160 class of coactivators. Because no direct p38 phosphorylation sites have been determined on either ERα or β, we hypothesized that p38 could target the p160 class of coactivators. We show for the first time using pharmacological and molecular techniques that the p160 coactivator glucocorticoid receptor interacting protein 1 (GRIP1) is phosphorylated and potentiated by the p38 MAPK signaling cascade *in vitro* and *in vivo*. S736 was identified as a necessary site for p38 induction of GRIP1 transcriptional activation. The C-terminus of GRIP1 was also demonstrated to contain a p38-responsive region. Taken together, these results indicate that p38 stimulates ER-mediated transcription by targeting the GRIP1 coactivator.

Introduction

Nuclear hormone receptors (NRs), such as the estrogen receptors (ERs), bind specific DNA response elements located in the promoter regions of target genes, thus driving transcription. Initiation of transcription requires the recruitment and binding of coactivators to specific regions located within the activation domains of the nuclear factors. For example, agonist bound ER forms a hydrophobic cleft in its AF-2 domain that recruits the p160 class of coactivators through specific LXXLL motifs located in the nuclear receptor interaction domain (NID) of the p160s (1). Furthermore, a C-terminal glutamine-rich region in the general coactivator p300/CREB-binding protein (CBP) binds the activation domain AD1 of p160s, creating a large coactivator complex that helps diverse nuclear transcription factors transcribe particular genes (2).

The p160 family of coactivators consists of three functionally similar proteins: steroid receptor coactivator-1 (SRC-1) (also known as nuclear coactivator 1 (N-CoA1) (3), glucocorticoid receptor interacting protein 1 (GRIP1) (also know as transcriptional intermediary factor 2 (TIF2), N-CoA2, and SRC-2) (1), and p300/CBP-interacting protein (p/CIP) (also known as activator of the thyroid and retinoic acid receptors (ACTR), receptor-associated coactivator 3 (RAC3), AIB1, thyroid hormone receptor activator molecule 1 (TRAM-1), SRC-3) (4). These coactivators help recruit histone acetyltransferases (p300/CBP) and methyltransferases (coactivator-associated arginine methyl-transferase-1 (CARM1)) to specific promoter regions, which combined with their own intrinsic histone acetyl transferase (HAT) activity, stimulate chromatin remodeling, recruit general transcription factors, and ultimately enhance gene expression (5). All three p160 members are able to significantly enhance liganded NR-mediated gene

expression. While much is known about how coactivators such as the p160s function to enhance transcription, relatively little is known about the regulation of these proteins.

Several labs have shown that kinase signaling cascades promote gene expression through the phosphorylation of coactivators. Protein kinase C (PKC), protein kinase A (PKA), and select CaM kinases can phosphorylate and potentiate CBP (6-9). Additionally, members of the MAPK signaling pathways including ERK, c-Jun N-terminal kinase (JNK), and MEK kinase 1 (MEKK1) phosphorylate and potentiate p300/CBP and the p160 coactivators SRC-1, GRIP1, and p/CIP (10-18).

p38 MAPK potentiates, in a ligand-inducible manner, nuclear hormone receptors such as the thyroid hormone receptor (TR), ERα, and ERβ as shown here and by others (19-22). However, no direct p38 phosphorylation sites have been determined. Additionally, interaction between TR and GRIP1 is synergistically potentiated by activation of p38 MAPK (21). Thus, we hypothesized that p38 MAPK phosphorylates and potentiates the p160 coactivator GRIP1. To test this hypothesis, we used dichlorodiphenyltrichloroethane (DDT), which we have previously shown activates p38 MAPK (23), as a pharmacological tool to determine if the p38 MAPK signaling cascade potentiates GRIP1. This data was supported using a variety of molecular mechanisms and pharmacological inhibitors. Finally, a combination of mammalian one-hybrid, *in vitro*, and *in vivo* kinase assays were used to test the ability of p38 MAPK to phosphorylate and stimulate GRIP1-mediated transcription.

Results

Constitutively active MKK6 enhances ERα- and β-mediated transcription. MAPK signaling cascades are known to regulate the ERs. For example, ERK can phosphorylate S118 of ERα, inducing ERα in a ligand-independent manner (24). JNK has previously been shown to potentiate ERα in an S118-independent mechanism (25). Here, we show both MCF-7 breast and Ishikawa endometrial carcinoma cells transfected with constitutively active MKK6, which selectively phosphorylates and activates p38 MAPK (26), enhances estrogen response element (ERE) activity treated with increasing amounts of E2 (Fig. 1). In MCF-7 cells this effect could be blocked by addition of a potent p38 inhibitor, RWJ67657 (27-29) (Fig. 2). Interestingly, RWJ67657 (10 μM) also inhibited vector transfected (VEC+Veh) cells, indicating that MCF-7 cells have basal p38 activity. This finding is consistent with our previous findings as well as the findings of other laboratories (30-32). Furthermore, using the anti-estrogens 4-OH-tamoxifen or ICI 182,780, we demonstrate the MKK6 enhancement of ERE-mediated transcription is ER-dependent (Fig. 3). Both anti-estrogens significantly inhibited MKK6 potentiation of E2-induced ERE activity. Human embryonic kidney (HEK) 293 cells, which do not contain functional ER, exhibit enhanced ERE-mediated transcription following transfection with expression plasmids for hERα (Fig. 4A) or hERβ (Fig. 4B) in conjunction with constitutively active MKK6, indicating the p38 MAPK cascade enhances ERα and ERβ activity.

Inhibition of p38 blocks estrogen-stimulated MCF-7 colony formation. To test the biological impact of p38 signaling on estrogen-mediated signaling, MCF-7 cells were treated with vehicle or E2 in combination with vehicle or RWJ67657 for 24 h. E2-treated

cells grew almost 200 colonies per test group over the following two weeks as compared to less than 115 colonies per group for cells treated with both E2 and RWJ67657 (Fig. 5). Cells treated with only RWJ67657 did decrease colony formation, consistent with our findings that MCF-7 cells have a basal level of p38 signaling. These data indicate p38 activity is required for normal growth in MCF-7 cells and inhibition of p38 activity leads to decreased MCF-7 cell proliferation.

The p38 MAPK signaling cascade activates GRIP1. Despite p38's ability to potentiate the ERs, no phosphorylation sites have ever been identified, raising the possibility that p38 may target ER-associated proteins such as GRIP1. To test this, constitutive active MKK mutants transfected into HEK 293 cells in conjunction with the GAL4-coactivator systems demonstrated that CA-MKK6 was the only MKK that significantly stimulated GRIP1 transcriptional activity (Fig. 6).

Previously, we demonstrated o,p'DDT, p,p'DDT, and o,p'DDT's metabolite, o,p'DDD, potently activate the p38 MAPK pathway. Hence, using the DDT congeners as pharmacological activators of p38, we exposed HEK 293 cells to o,p'DDT, p,p'DDT, or o,p'DDD. Treatment with these compounds lead to the potentiation of GAL4 fusion proteins of full length GRIP1, but not empty GAL4 expression vector (Fig. 7A). To demonstrate that DDT-induced coactivator activity is mediated through p38, we blocked o,p'DDT-stimulated coactivator activity with both molecular and pharmacological inhibitors of the various MAPK pathways. HEK 293 cells were transfected with increasing amounts of dominant negative (DN) ERK2, JNK1, or p38α along with a GAL4 reporter-plasmid and full length GAL4-GRIP1 chimera followed by treatment with vehicle (DMSO) or 50 μM o,p'DDT. DN-p38α, and to a lesser degree DN-ERK2,

but not DN-JNK1, inhibited DDT-induced GRIP1 activity (Fig. 7, B and C). All inhibitory effects were significantly greater ($p < 0.05$) in o,p'DDT treated cells versus vehicle treated cells. DN-p38α, significantly inhibited ($p < 0.001$) o,p'DDT-induced GRIP1 activity 50-60%.

To confirm our molecular inhibitory findings, we blocked DDT-induced coactivator activity with pharmacological inhibitors of the MAPK pathways. GAL4 empty expression vector or GAL4-GRIP1 was transfected into HEK 293 cells and treated with vehicle or different MAPK inhibitors for 1 h, followed by treatment with vehicle or 50 μM o,p'DDT. The p38 pharmacological inhibitor SB203580 significantly blocked ($p < 0.001$) o,p'DDT induction GRIP1, whereas there was no effect on cells transfected with empty GAL4 expression plasmid (Fig. 7D). Surprisingly, both U0126 and SP600125 also inhibited ($p < 0.001$) DDT-induced GRIP1 activity, indicating multiple MAPKs may converge on GRIP1. Collectively, these data confirm that DDT activates the transcriptional coactivator GRIP1 via the p38 MAPK pathway.

p38 phosphorylates GRIP1 in vitro and in vivo. Recent reports have demonstrated various kinases, including the MAPKs ERK and JNK, can potentiate coactivators such as p300/CBP and p160 coactivators through phosphorylation (6-9, 12-14, 16-18). We hypothesized that p38 MAPK phosphorylates GRIP1, leading to its potentiation. To test this hypothesis *in vitro*, we bacterially expressed a recombinant GRIP1 fragment using GST purification. Western blots using antibodies against GST revealed GST-fusion proteins broke down into smaller fragments (data not shown), consistent with what others have seen (16). A map of the GST-fusion proteins tested is shown in Fig. 8A. Purified fusion proteins were then subjected to an *in vitro* kinase assay

in the presence of ^{32}P and activated p38 MAPK. The GST-GRIP1 fusion protein fragment containing amino acids 184-766, which has previously been reported to be responsive to ERK phosphorylation, was also phosphorylated by activated p38 MAPK (Fig. 8B). Our negative control, GST alone, was not phosphorylated by p38 MAPK. However, our positive control, a GST fusion protein containing MAPKAPK-2, a bona fide p38 substrate, was phosphorylated by p38 *in vitro*.

To show that phosphorylation of GRIP1 protein is regulated by p38 MAPK *in vivo*, a GAL4-GRIP1-NRID (aa 5-756) expression vector was transfected into COS-1 cells using an adenovirus-mediated DNA transfer technique to increase protein expression. High-level expression in COS-1 cells was necessary to visualize phosphorylated GRIP1 as expression of GAL4-GRIP1-NRID in 293 cells yielded insufficient protein to visualize a [^{32}P]-labeled phosphorylated band. Following *in vivo* labeling of cells with [^{32}P]H_3PO_4 and incubation with SB203580 (SB), o,p'DDT (DDT), or SB+DDT, an immunopurified GAL4-GRIP-NRID protein band was visualized by Western blot and autoradiography. Incubation with SB resulted in a reproducible decrease in GRIP1 phosphorylation whereas DDT treatment increased GRIP1 phosphorylation. Combined incubation of DDT+SB abrogated the increased GRIP1 phosphorylation by DDT (Fig. 9A, upper panel). Western blot for Gal-GRIP-NRID with the identical membrane shown directly below the autoradiogram (Fig. 9A, lower panel) was used to normalize the relative change in GRIP1 phosphorylation due to SB and DDT treatments (Fig. 9B). Remarkably, the relative level of GRIP1 phosphorylation regulated by SB and DDT was directly correlated to the relative activity of GRIP1 induced by these

two agents, singly or in combination (see Fig. 7). Taken together, these data demonstrate for the first time that p38 MAPK phosphorylates the coactivator GRIP1.

Identification of sites of GRIP1 involved in p38 responsiveness. To determine the specific regions p38 potentiates and to compliment our kinase data, we transfected HEK 293 cells as before with either empty expression vector or CA-MKK6 for 6 h in conjunction with GAL4-coactivator systems using GAL4-GRIP1 fragment and site mutant constructs. A map of the GAL4-protein fusions is shown in Fig. 10A. Cells were then treated with vehicle or o,p'DDT (50 μM) overnight. Hence, p38 was stimulated both by molecular (CA-MKK6) and pharmacological (o,p'DDT) means. Both CA-MKK6 and o,p'DDT were able to potentiate full length GAL4-GRIP1 as expected. However, both CA-MKK6 and o,p'DDT were unable to potentiate GAL4-GRIP1 when the putative MAPK phosphorylation site S736 (18) was mutated to an alanine (Fig. 10B). This data supports our GRIP1 kinase data that used GST-GRIP1 and GAL4-GRIP fragments that encompassed S736. Also, potentiation of p38 stimulated a GAL4-GRIP1 fragment containing amino acids 730-1121, which contains the S736 site. Additionally though, both CA-MKK6 and o,p'DDT significantly potentiated ($p < 0.05$ and $p < 0.001$, respectively) the GAL4-GRIP1 fragment containing the C-terminal region of amino acids 1121-1462, indicating that another, more C-terminal, p38 target site exists. Thus, our kinase data strongly correlates with the GAL4 studies, but suggests that other potential p38 phosphorylation sites most likely exist. S736, as well as an unknown C-terminal site(s) are targeted by the p38 MAPK signaling cascade.

Next, to confirm whether S736 is a major site for p38 MAPK-regulated phosphorylation *in vivo*, GAL4-GRIP1-NRID-S736A was transfected into COS-1 cells

using the adenovirus-mediated DNA transfer technique followed by *in vivo* labeling with [^{32}P] H_3PO_4 and overnight incubation with vehicle, SB, DDT or SB+DDT. Vehicle-treated wild type GAL4-GRIP1-NRID and mutant GAL4-GRIP1-NRID-S736A were also transfected and labeled with [^{32}P] H_3PO_4 to compare differences in phosphorylation levels. Compared to wild type (GAL4-GRIP1-NRID), the phosphorylation level of GAL4-GRIP1-NRID-S736A was significantly lower ($p < 0.05$) (Fig. 11), consistent with our earlier findings that indicate there is a basal p38 phosphorylation of GRIP1 (Figs 2, 5, 9) (23). However, when the GAL4-GRIP1-NRID-S736A mutant transfected cells were treated with p38 inhibitor (SB), p38 activator (DDT), or SB+DDT no significant change was observed in the normalized phosphorylation levels of treated cells (Fig. 11) unlike wild type GAL4-GRIP1-NRID (Fig. 9).

Finally, we directly linked the suspected p38 target site S736 to ER-mediated transcription. MCF-7 cells stably expressing either empty expression vector or CA-MKK6 were transiently transfected with pERE-Luc and empty, wild-type GRIP1, or GRIP1 S736A expression vectors and treated with vehicle or E2 (100 pM). CA-MKK6 potentiated ERE-mediated transcription in GRIP1 transfected cells, an effect that was increased upon E2 treatment (Fig. 12). However, in agreement with our GAL4-GRIP1 data (see Figs. 10+11), mutation of S736 blocks the MKK6 stimulation of ERE-mediated gene transcription to empty expression vector transfected levels, an effect not seen in the MCF-7-Vec cell line. Previously, we demonstrated that mutation of serine 736 to an alanine does not affect the expression or the localization of GRIP1 (18). Collectively, these findings indicate the MKK6-p38 MAPK signaling cascade increases ER-mediated expression through S736 of GRIP1.

Discussion

Coactivators are critical components involved in the process of transcriptional initiation and elongation. The p160 coactivator GRIP1 is needed for normal reproductive behavior and function, in addition to playing a major role in lipid metabolism and energy balance (5). Thus, determining the regulation of this coactivator is central to understanding how signaling mechanisms control gene expression and ultimately biological function. Here, we demonstrate that the p38 MAPK signaling cascade phosphorylates and potentiates the nuclear coactivator GRIP1.

p38 was shown to target the ERs. We stimulated ER-mediated transcription by potentiating the p38-signaling cascade and blocked this potentiation using the p38 inhibitor RWJ67657 (Figs. 1-3,12). Additionally, we also demonstrated that inhibition of p38 signaling blocks estrogen-induced MCF-7 cell proliferation (Fig. 5). However, how p38 potentiated the ERs was unexplained (19, 20). Steroid hormone receptors recruit common coactivators (2, 5), indicating that perhaps p38 signaling to the NRs could be explained by an indirect potentiation, one favoring the shared coactivators. Mammalian one-hybrid assays using GAL4-GRIP1 constructs demonstrate constitutively active MKK6 significantly increased GRIP1 activity (Fig. 6). In addition, o,p'DDT, p,p'DDT, and o,p'DDD, which all were previously shown to stimulate p38 activity (23), stimulated GRIP1 transcriptional activity (Fig. 7A). Another DDT metabolite found in humans, p,p'DDA, which does not affect p38 signaling (23), likewise had no effect on GRIP1 activity. While DDT was used primarily as a pharmacological tool to stimulate p38

activity, these data also represent a novel mechanism by which environmental compounds can mediate transcriptional regulation.

Contrary to the effects of DDT alone, both a dominant negative mutant and a pharmacological inhibitor of p38 (SB203580), blocked DDT-induced GRIP1 signaling (Figs. 7B-D,9). This potentiation also appeared to be due, in part, to the ERK signaling cascade, although to a lower degree. ERK has previously been demonstrated to potentiate the p160s (12, 14, 17, 18). Here, we demonstrate for the first time that p38 targets GRIP1. These data explain the findings that p38 potentiates ERα and β, despite the presence of a known p38 phosphorylation site on the ERs (19, 20).

Sequence analysis indicates several possible p38 MAPK sites in GRIP1. We demonstrated *in vitro* and *in vivo* that p38 leads to the phosphorylation of GRIP1 (Figs. 8 and 9). A fragment of GRIP1 containing amino acids 184-766 was previously demonstrated to be ERK responsive (18). This same region is also phosphorylated by the p38 MAPK. We believe this roughly 2-fold phosphorylation *in vivo* is highly significant. Proteins are multiply phosphorylated *in vivo* and it is likely that only one or at most a few of the phosphorylation sites in GRIP1 are actually responsible for the functional activity of GRIP1. Hence, if p38 alters phosphorylation of only one site in a multiply phosphorylated protein and this one site is critical for function, then the overall phosphorylation of GRIP1 will not be greatly altered. Functional analysis demonstrates S736, which is also targeted by ERK (18), is necessary for p38 induction of GRIP1 activity (Figs. 10+11) and ER-mediated transcription (Fig. 12). Insight can also be obtained from the breakdown products of the GST fusion proteins. Western blots using antibodies against GST demonstrate that the fusion proteins breakdown on the C-terminal

side, opposite GST, since the GST bands can be detected all the way down to a fragment roughly the size of GST alone (data not shown). Phosphorylation by p38 at only the largest GST-GRIP fusion protein products supports the idea that a site at the extreme C-terminus of my fusion protein fragment is phosphorylated. This would support S736 as a likely phosphorylation site. This site is located in the NID and may play a role in nuclear receptor recruitment of GRIP1. A GAL4-GRIP1 fusion protein containing amino acids 730-1121 was stimulated by both o,p'DDT and CA-MKK6, further supporting the region containing S736 is stimulated by p38. Although, we can not rule out that other sites in this region may also be targeted. Interestingly, S736 is not conserved in any of the other p160 coactivators, indicating GRIP1 may be regulated differently than other homologous proteins. However, p38 regulation of the other p160s remains unknown. Whether S736 is directly phosphorylated by p38 MAPK requires further biochemical analysis. Additionally, o,p'DDT and CA-MKK6 were both able to potentiate a C-terminal fragment of GRIP1 containing amino acids 1121-1462 (Fig. 10). These data indicate another p38-responsive region exists in the C-terminus of GRIP1. The related p160 coactivator, SRC-1, was previously reported to be phosphorylated and activated on several C-terminal sites (14). However, none of the targeted sites appear to be conserved in GRIP1. But, there are predicted p38 sites at T1318, S1321, and S1325. These sites all lie in the AD2 domain of GRIP1 that is responsible for recruitment of the methyltransferase coactivator CARM1 (33, 34). Thus, p38 potentiation of the GRIP1 C-terminus may lead to recruitment of CARM1.

Our results demonstrate a novel mechanism for p38-induced transcription. Transcription factors such as Elk1, activating transcription factor 2 (ATF2), and ER are

all convergent points for p38 signaling pathways (22, 35, 36). Some transcription factors such as Elk1 and ATF2 are directly phosphorylated by p38 (36, 37). Here, we show another level of p38-transcriptional regulation, p38 targeting of the recruited coactivator GRIP1. This added requirement may help p38 selectively activate target genes.

Materials and Methods

Chemicals. o,p'DDT, p,p'DDT, o,p'-dichlorodiphenyldichloroethane (DDD), and p,p'-dichlorodiphenyl acetic acid (DDA) were purchased from AccuStandard (New Haven, CT). All DDT metabolites were dissolved in dimethyl sulfoxide (DMSO). 17β-estradiol (E2), 4-OH-tamoxifen, and tetradecanoyl-13-phorbol acetate (PMA) were purchased from Sigma and dissolved in DMSO or DMEM respectively. U0126 (MAPK/ERK kinase (MEK)1/2 inhibitor) was purchased from Promega (Madison, WI). SP600125 (JNK inhibitor) was purchased from BIOMOL Research Laboratories Inc. (Plymouth Meeting, PA). SB203580 (p38 inhibitor) was purchased from Calbiochem (San Diego, CA). RWJ67657 (p38 inhibitor) was a gift from Johnson and Johnson Pharmaceutical Research and Development, L.L.C. (Raritan, NJ). ICI 182,780 was purchased from ICI 182,780 was purchased from TOCRIS (Ballwin, MO). All pharmacological inhibitors were dissolved in DMSO.

Cell culture and transient transfection. MCF-7, Ishikawa, and HEK 293 cells were grown as previously described (23, 38-40). Cultures of cells were transferred to phenol red-free DMEM supplemented with 5% dextran coated charcoal-stripped-FBS (DCC-FBS), BME amino acids, MEM non-essential amino acids, sodium pyruvate, and penicillin-streptomycin for 24 h prior to plating. Cells were plated at a density of 5×10^5

cells/well in 24-well plates (approximately 80% confluency) and maintained for an additional 24 h in DMEM with 5% DCC-FBS.

For ERE assays MCF-7, Ishikawa, or HEK 293 cells (Figs. 1-4) were then transfected for 4-6 h as indicated in figure legend with 100 ng of pERE-Luc using Effectene (Qiagen) according to the manufacturer's protocol in combination with 200 ng pcDNA3-CA-MKK6b (CA-MKK6; constitutive active) or empty expression vector. HEK 293 cells were additionally transfected with 50 ng of pcDNA3.1-hERα or pcDNA3.1-hERβ expression plasmids.

For ERE assays in stably transfected MCF-7 cells (Fig. 11), cells were transfected for 5 h with 300 ng of pERE-Luc and 200 ng of empty pSG5, pSG5-GRIP1 full-length, or pSG5-GRIP1 S736A using Effectene in a 20:1 ratio (μl lipid: μg DNA) according to the manufacturer's instructions.

For GAL4 one-hybrid assays, 50 ng of pFR-Luc (Stratagene, La Jolla, CA) was transfected with FuGENE 6^{TM} lipofection reagent according to the manufacturer's protocol for 6 h in combination with 25 ng of CMV-GAL4 (negative control), 200 ng GAL4-GRIP1 full length (aa: 5-1462), GAL4-GRIP1 (aa: 730-1121), GAL4-GRIP1 (aa: 1121-1462) (Michael Stallcup, University of Southern California), or GAL4-GRIP1 S736A (previously been described (18)) with or without 100 ng pcDNA3.1 expression vector (Invitrogen, Carlsbad, CA), pFC-MEK1 (CA-MKK1; constitutive active MKK1) (Stratagene), pcDNA3-CA-MKK5 (constitutive active) (Jiing-Dwan Lee, Scripps Research Institute), pcDNA3-CA-MKK6b, or pcDNA3-CA-MKK7 (constitutive active) (Jiahuai Han, Scripps Research Institute) as indicated. CA-MKK1, CA-MKK6, and CA-MKK7 were previously demonstrated to activate Elk-1, ATF2, and c-Jun respectively,

known targets of ERK, p38, and JNK MAPKs (26, 41-44). CA-MKK5 has previously been shown to phosphorylate and potentiate BMK1 (45). Cytomegalovirus (CMV) promoters drove all expression vectors.

For dominant negative experiments, HEK293 cells were transfected with FuGENE 6^{TM} lipofection reagent according to the manufacturer's protocol for 24 h using 50 ng of pFR-Luc (Stratagene) and 200 ng GAL4-GRIP1 full length in conjunction with 0, 50, 100, or 150 ng of dominant negative mutant plasmid. Total DNA volume was brought up, if necessary, using empty pcDNA3.1 expression vector. MAPK dominant negative mutants were kindly provided by Jiing-Dwan Lee (Scripps Research Institute, La Jolla, CA) (ERK2) and Roger Davis (University of Massachusetts Medical School, Worcester, MA)(JNK1 and p38α). CMV promoters drove all dominant negative mutant expression vectors.

Reporter gene assay. For all luciferase assays, transfected cells were incubated for 18-24 h in DMEM with 5% DCC-FBS in the presence of vehicle or various chemicals as previously described (23, 39). Where indicated, inhibitors were added 1 h prior to the addition of DMSO, E2, PMA, or DDT metabolites and maintained during the remainder of the incubation period. Inhibitor concentrations were chosen based on non-toxic levels, published IC_{50} values from manufacturers, and previous experiments demonstrating inhibition of known MAPK signaling pathways (27-30) and unpublished data. In our results we have shown the data from treatments using 25-50 μM DDT and its metabolites, which gave significant p38 activity as previously demonstrated (23). Finally, cells were harvested and luciferase activity was measured using 30 μl of cell extract and 100 μl of Luciferase Assay Substrate (Promega) in a Berthold AutoLumat

Plus luminometer. The data shown are an average of at least three independent experiments with two replicates.

Colony Assay. MCF-7 cells were plated in 6 well plates at 1,000 cells per well in DMEM with 5% DCC-FBS. The following day the cells were pre-treated with DMSO or RWJ67657 at 10μM followed by either DMSO or E2 (1nM). The cells were then monitored microscopically for colony growth. The cells were fixed by adding glutaraldehyde (2.5% final concentration) directly to the well. 15 to 30 minutes later the plates were washed and stained with a 0.4% solution of crystal violet in 20% methanol for 15 to 30 minutes. The crystal violet solution was removed and the plates washed and dried. Colonies with a cell confluence of 50 or greater were counted.

GST fusion protein purification. The glutathione-S-transferase (GST) and GST-coactivator fusion proteins were generated using pGEX empty GST expression vector (Amersham Biosciences, Piscataway, NJ) or pGEX-GRIP1 (aa: 184-766) (Michael Stallcup, University of Southern California) transformed into BL21star cells (Invitrogen). Bacteria were grown overnight in LB supplemented with 50 μg/ml ampicillin at 37°C with shaking. The following morning, bacteria was diluted 1:100 in fresh LB supplemented media and grown at 37°C to an A_{600} = .5-2. Protein expression was then induced for 3 h with 0.1M isopropyl-β-D-thiogalactopyranoside (IPTG). After induction, cells were collected by centrifugation at 7500 x g for 10 min at 4°C. The supernatant was discarded; the pellet was resuspended in cold 1X PBS supplemented with .1 mM phenylmethylsulfonyl fluoride (PMSF) and 10 μl protease inhibitor cocktail for use with bacterial cell lysates (Sigma). Resuspensions were frozen overnight at –80°C. The following morning, suspensions were thawed and then sonicated mildly twice for 45 sec.

20% Triton X-100 was added to the suspensions to a final concentration of 1% and mixed gently for 30 min to help solubilize the fusion proteins. The suspensions were then centrifuged at 12,000 x g for 10 min at 4°C. The supernatants were transferred to fresh tubes and GST fusion proteins were purified using the Bulk GST Purification Module (Amersham Biosciences) according to the manufacturer's protocol.

In vitro kinase assay. Roughly 3-5 μg of eluted purified GST fusion protein or 200 ng of purified MAPK activated protein kinase-2 (MAPKAPK-2) (Upstate Biotechnology, Lake Placid, NY) was then incubated for 30 min at 30°C with shaking with 0.06U of activated p38α (Upstate Biotechnology, Lake Placid, NY) in the presence of Magnesium/ATP cocktail containing [γ-^{32}P] (Upstate Biotechnology, Lake Placid, NY) according to the manufacturer's protocol. Reactions were stopped by the addition of 20 μl 2X SDS sample buffer containing .1M PMSF, protease inhibitor cocktail, phosphatase inhibitor cocktail (Sigma), and β-mercaptoethanol and boiling samples for 5 min. Samples were analyzed by 4-12% SDS-PAGE (Invitrogen), stained with coomassie blue to monitor expression, and subjected to autoradiography.

Western blot. Western blots were performed as previously described using approximately 50 μg of crude bacterial lysate or 10 μg of purified GST fusion proteins analyzed by 4-12% SDS-PAGE. Proteins were transferred to nitrocellulose membranes and probed using a 1:1000 dilution of Goat anti-GST antibody (Amersham Biosciences) in blocking solution followed by rabbit anti-goat peroxidase labeled antibody (1:2500 dilution in blocking solution) (Kirkegaard and Perry Laboratories, Gaithersburg, MD).

In vivo phosphorylation of GAL4-GRIP1-NRID and GAL4-GRIP1-NRID-S736A. 4 x 10^6 COS-1 cells were plated onto 150 mm dishes in DMEM with 5% DCC-

FBS. After 24 h incubation, the cells were transfected with GAL4-GRIP1-NRID or GAL4-GRIP1-NRID-S736A using a non-recombinant adenovirus DNA transfer procedure. Briefly, plasmid DNA (100 ng/plate) was mixed with polylysine-coupled adenovirus and incubated for 30 min at room temperature. Before the addition of the adenovirus-plasmid particles to the cells, the medium was aspirated and replaced with serum-free DMEM. The adenovirus-plasmid particles were added to the cells at a 400:1 adenovirus:cell ratio and incubated for 2 h at 37°C. After incubation, an equal volume of DMEM with 5% DCC-FBS was added to each dish resulting in a final concentration of 2.5% DCC-FBS. 24 h after transfection, the medium was aspirated from the dishes and replaced with phosphate-free, serum-free DMEM, and the cells were incubated for 1 h at 37°C. The medium was removed and replaced with phosphate free DMEM-containing 1% dialyzed FBS before the addition of 0.27 mCi/ml $[^{32}P]H_3PO_4$. 1 h after addition of $[^{32}P]H_3PO_4$, cells were incubated with either vehicle, 6 μM SB203580, 25 μM o,p'DDT, or 6 μM SB203580 + 25 μM o,p'DDT. Three plates were used for each treatment. Cells were incubated for 15 h at 37°C. Following this incubation, the medium was aspirated, the cells were rinsed two times with PBS, and the cells were collected by scraping and centrifugation. The cell pellet was then incubated with lysis buffer (10 mM Tris (pH 8.0), 0.4 M NaCl, 1 mM EDTA, 1 mM EGTA, 10 mM β-mercaptoethanol, 0.1% Triton-X-100, and cocktail protease inhibitor (Sigma)) for 10 min with vortexing and centrifuged at 16,000 rpm for 10 min at 4°C. Protein A-sepharose beads (Amersham Biosciences) were incubated with 2 μg of antibody to the GAL4 DNA binding domain (sc-577; Santa Cruz Biotechnology, Santa Cruz, CA) for 1 h at room temperature and then incubated with the cell lysate supernatant for 2 h while rotating at 4°C. As a

negative control with respect to the GAL4 antibody, which was used in the IP to isolate the GAL4-GRIP1-NRID protein, a separate three plates of ^{32}P-labeled vehicle-treated GAL4-GRIP1-NRID transfected COS-1 cells were also harvested and incubated with lysis buffer for 10 min with vortexing, followed by centrifugation at 16,000 rpm for 10 min at 4°C. The cell lysate supernatant was incubated for 2 h at 4°C with normal mouse IgG (sc-2025, Santa Cruz Biotechnology) bound protein A sepharose beads. Before adding the cell lysate, protein A beads were incubated with normal mouse IgG for 1 h at room temperature. The beads of all samples were washed with 100 volumes of cold PBS followed by addition of Laemmli sample buffer. After boiling for 5 min, the samples were electrophoresed on a 10% SDS-polyacrylamide gel and transferred to a nitrocellulose membrane for autoradiography for approximately 30 minutes. The same membrane was subsequently used for Western blotting to detect GAL4-GRIP-NRID or GAL4-GRIP1-NRID-S736A using a horseradish peroxidase-conjugated antibody to the GAL4 DNA binding domain (sc-510HRP; Santa Cruz Biotechnology). The Western blot signal was developed with enhanced chemiluminescenc (ECL). Autoradiography signals were quantitated by densitometric scanning of films and ECL signals were quantitated using a Kodak Image Station 440CF.

Creation of MCF-7-Vector and MCF-7-MKK6b(CA) stably transfected cell lines. MCF-7 cells were plated at 5x10^6 cells in 100 mm dishes in DMEM medium with 10% FBS and incubated overnight at 5% CO_2 and 37°C. The next morning 30 µl of FuGENE 6^{TM} reagent was added to 5 ml of Opti-MEM (Invitrogen) and gently mixed and incubated at room temperature for 5 min. To this mixture were added 10 µg pcDNA3.0 or pcDNA3.0-MKK6b(E) constitutive active mutant. After gently mixing, this solution was

incubated at room temperature for 30 min. The transfection mix was added to the 100 mm dish drop-wise and incubated overnight at 5% CO_2 and 37°C. The next day the media was changed and geneticin (Invitrogen) was added to the fresh media at a final concentration of 200 μg/ml. The dish was incubated overnight at 5% CO_2 and 37°C. Over the next two weeks the cells were checked for cell death of non-transfected cells and colonies of surviving cells were harvested and expanded. Presence of functional CA-MKK6 was verified by Western blot analysis of phosphorylated p38 (data not shown).

Statistical analysis. Data was analyzed using one-way ANOVA and post hoc Tukey's multiple comparisons with GraphPad Prism, Version 3.02 (GraphPad Software, Inc.). Statistically significant changes were determined at the $p < 0.05$, $p < 0.01$, or $p < 0.001$ level as indicated for each figure or table.

Acknowledgements

We thank Dr. Scott Wadsworth and Johnson & Johnson for generous provision of RWJ67657 used in this study.

References

1. Hong H, Kohli K, Garabedian M, Stallcup M 1997 GRIP1, a transcriptional coactivator for the AF-2 transactivation domain of steroid, thyroid, retinoid, and vitamin D receptors. Mol Cell Biol 17:2735-2744

2. Goodman RH, Smolik S 2000 CBP/p300 in cell growth, transformation, and development. Genes Dev 14:1553-1577

3. Onate SA, Tsai SY, Tsai MJ, O'Malley BW 1995 Sequence and characterization of a coactivator for the steroid hormone receptor superfamily. Science 270:1354-1357.

4. Torchia J, Rose DW, Inostroza J, Kamei Y, Westin S, Glass CK, Rosenfeld MG 1997 The transcriptional co-activator p/CIP binds CBP and mediates nuclear-receptor function. Nature 387:677-684.

5. Xu J, Li Q 2003 Review of the in vivo functions of the p160 steroid receptor coactivator family. Mol Endocrinol 17:1681-1692

6. Zanger K, Radovick S, Wondisford FE 2001 CREB binding protein recruitment to the transcription complex requires growth factor-dependent phosphorylation of its GF box. Mol Cell 7:551-558

7. Swope DL, Mueller CL, Chrivia JC 1996 CREB-binding protein activates transcription through multiple domains. J Biol Chem 271:28138-28145

8. Hu SC, Chrivia J, Ghosh A 1999 Regulation of CBP-mediated transcription by neuronal calcium signaling. Neuron 22:799-808

9. Hardingham GE, Chawla S, Cruzalegui FH, Bading H 1999 Control of recruitment and transcription-activating function of CBP determines gene regulation by NMDA receptors and L-type calcium channels. Neuron 22:789-798

10. Janknecht R, Nordheim A 1996 MAP kinase-dependent transcriptional coactivation by Elk-1 and its cofactor CBP. Biochem Biophys Res Commun 228:831-837

11. Sang N, Stiehl DP, Bohensky J, Leshchinsky I, Srinivas V, Caro J 2003 MAPK signaling up-regulates the activity of hypoxia-inducible factors by its effects on p300. J Biol Chem 278:14013-14019

12. Ueda T, Mawji NR, Bruchovsky N, Sadar MD 2002 Ligand-independent activation of the androgen receptor by interleukin-6 and the role of steroid receptor coactivator-1 in prostate cancer cells. J Biol Chem 277:38087-38094

13. Rowan BG, Garrison N, Weigel NL, O'Malley BW 2000 8-Bromo-cyclic AMP induces phosphorylation of two sites in SRC-1 that facilitate ligand-independent activation of the chicken progesterone receptor and are critical for functional cooperation between SRC-1 and CREB binding protein. Mol Cell Biol 20:8720-8730

14. Rowan BG, Weigel NL, O'Malley BW 2000 Phosphorylation of steroid receptor coactivator-1. Identification of the phosphorylation sites and phosphorylation through the mitogen- activated protein kinase pathway. J Biol Chem 275:4475-4483.

15. Gusterson R, Brar B, Faulkes D, Giordano A, Chrivia J, Latchman D 2002 The transcriptional co-activators CBP and p300 are activated via phenylephrine through the p42/p44 MAPK cascade. J Biol Chem 277:2517-2524

16. See RH, Calvo D, Shi Y, Kawa H, Luke MP, Yuan Z 2001 Stimulation of p300-mediated transcription by the kinase MEKK1. J Biol Chem 276:16310-16317

17. Font de Mora J, Brown M 2000 AIB1 Is a Conduit for Kinase-Mediated Growth Factor Signaling to the Estrogen Receptor. Mol Cell Biol 20:5041-5047

18. Lopez GN, Turck CW, Schaufele F, Stallcup MR, Kushner PJ 2001 Growth factors signal to steroid receptors through mitogen-activated protein kinase regulation of p160 coactivator activity. J Biol Chem 276:22177-22182.

19. Lee H, Jiang F, Wang Q, Nicosia SV, Yang J, Su B, Bai W 2000 MEKK1 activation of human estrogen receptor alpha and stimulation of the agonistic activity of 4-hydroxytamoxifen in endometrial and ovarian cancer cells. Mol Endocrinol 14:1882-1896.

20. Driggers PH, Segars JH, Rubino DM 2001 The proto-oncoprotein Brx activates estrogen receptor beta by a p38 mitogen-activated protein kinase pathway. J Biol Chem 276:46792-46797.

21. Chen SL, Chang YJ, Wu YH, Lin KH 2003 Mitogen-activated protein kinases potentiate thyroid hormone receptor transcriptional activity by stabilizing its protein. Endocrinology 144:1407-1419

22. Lee H, Bai W 2002 Regulation of estrogen receptor nuclear export by ligand-induced and p38-mediated receptor phosphorylation. Mol Cell Biol 22:5835-5845

23. Frigo DE, Tang Y, Beckman BS, Scandurro AB, Alam J, Burow ME, McLachlan JA 2004 Mechanism of AP-1-mediated gene expression by select organochlorines through the p38 MAPK pathway. Carcinogenesis 25:249-261

24. Kato S, Endoh H, Masuhiro Y, Kitamoto T, Uchiyama S, Sasaki H, Masushige S, Gotoh Y, Nishida E, Kawashima H, et al. 1995 Activation of the estrogen receptor through phosphorylation by mitogen- activated protein kinase. Science 270:1491-1494.

25. Feng W, Webb P, Nguyen P, Liu X, Li J, Karin M, Kushner PJ 2001 Potentiation of estrogen receptor activation function 1 (AF-1) by Src/JNK through a serine 118-independent pathway. Mol Endocrinol 15:32-45.

26. Jiang Y, Chen C, Li Z, Guo W, Gegner JA, Lin S, Han J 1996 Characterization of the structure and function of a new mitogen-activated protein kinase (p38beta). J Biol Chem 271:17920-17926

27. Wadsworth SA, Cavender DE, Beers SA, Lalan P, Schafer PH, Malloy EA, Wu W, Fahmy B, Olini GC, Davis JE, Pellegrino-Gensey JL, Wachter MP, Siekierka JJ 1999 RWJ 67657, a potent, orally active inhibitor of p38 mitogen-activated protein kinase. J Pharmacol Exp Ther 291:680-687

28. Fijen JW, Zijlstra JG, De Boer P, Spanjersberg R, Tervaert JW, Van Der Werf TS, Ligtenberg JJ, Tulleken JE 2001 Suppression of the clinical and cytokine response to endotoxin by RWJ-67657, a p38 mitogen-activated protein-kinase inhibitor, in healthy human volunteers. Clin Exp Immunol 124:16-20

29. Faas MM, Moes H, Fijen JW, Muller Kobold AC, Tulleken JE, Zijlstra JG 2002 Monocyte intracellular cytokine production during human endotoxaemia with or

without a second in vitro LPS challenge: effect of RWJ-67657, a p38 MAP-kinase inhibitor, on LPS-hyporesponsiveness. Clin Exp Immunol 127:337-343

30. Alam J, Wicks C, Stewart D, Gong P, Touchard C, Otterbein S, Choi AM, Burow ME, Tou J 2000 Mechanism of heme oxygenase-1 gene activation by cadmium in MCF-7 mammary epithelial cells. Role of p38 kinase and Nrf2 transcription factor. J Biol Chem 275:27694-27702.

31. Tsai PW, Shiah SG, Lin MT, Wu CW, Kuo ML 2003 Up-regulation of vascular endothelial growth factor C in breast cancer cells by heregulin-beta 1. A critical role of p38/nuclear factor-kappa B signaling pathway. J Biol Chem 278:5750-5759

32. Alsayed Y, Uddin S, Mahmud N, Lekmine F, Kalvakolanu DV, Minucci S, Bokoch G, Platanias LC 2001 Activation of Rac1 and the p38 mitogen-activated protein kinase pathway in response to all-trans-retinoic acid. J Biol Chem 276:4012-4019

33. Ma H, Hong H, Huang SM, Irvine RA, Webb P, Kushner PJ, Coetzee GA, Stallcup MR 1999 Multiple signal input and output domains of the 160-kilodalton nuclear receptor coactivator proteins. Mol Cell Biol 19:6164-6173

34. Chen D, Ma H, Hong H, Koh SS, Huang SM, Schurter BT, Aswad DW, Stallcup MR 1999 Regulation of transcription by a protein methyltransferase. Science 284:2174-2177

35. Chen Z, Raman M, Chen L, Lee SF, Gilman AG, Cobb MH 2003 TAO (thousand-and-one amino acid) protein kinases mediate signaling from carbachol

to p38 mitogen-activated protein kinase and ternary complex factors. J Biol Chem 278:22278-22283

36. Ouwens DM, de Ruiter ND, van der Zon GC, Carter AP, Schouten J, van der Burgt C, Kooistra K, Bos JL, Maassen JA, van Dam H 2002 Growth factors can activate ATF2 via a two-step mechanism: phosphorylation of Thr71 through the Ras-MEK-ERK pathway and of Thr69 through RalGDS-Src-p38. Embo J 21:3782-3793

37. Bebien M, Salinas S, Becamel C, Richard V, Linares L, Hipskind RA 2003 Immediate-early gene induction by the stresses anisomycin and arsenite in human osteosarcoma cells involves MAPK cascade signaling to Elk-1, CREB and SRF. Oncogene 22:1836-1847

38. Collins-Burow BM, Burow ME, Duong BN, McLachlan JA 2000 Estrogenic and antiestrogenic activities of flavonoid phytochemicals through estrogen receptor binding-dependent and -independent mechanisms. Nutr Cancer 38:229-244

39. Frigo DE, Burow ME, Mitchell KA, Chiang TC, McLachlan JA 2002 DDT and Its Metabolites Alter Gene Expression in Human Uterine Cell Lines through Estrogen Receptor-Independent Mechanisms. Environ Health Perspect 110:1239-1245.

40. Frigo DE, Duong BN, Melnik LI, Schief LS, Collins-Burow BM, Pace DK, McLachlan JA, Burow ME 2002 Flavonoid Phytochemicals Regulate Activator Protein-1 Signal Transduction Pathways in Endometrial and Kidney Stable Cell Lines. J Nutr 132:1848-1853.

41. Wong BR, Josien R, Lee SY, Vologodskaia M, Steinman RM, Choi Y 1998 The TRAF family of signal transducers mediates NF-kappaB activation by the TRANCE receptor. J Biol Chem 273:28355-28359

42. Fantz DA, Jacobs D, Glossip D, Kornfeld K 2001 Docking sites on substrate proteins direct extracellular signal-regulated kinase to phosphorylate specific residues. J Biol Chem 276:27256-27265

43. Alpert D, Schwenger P, Han J, Vilcek J 1999 Cell stress and MKK6b-mediated p38 MAP kinase activation inhibit tumor necrosis factor-induced IkappaB phosphorylation and NF-kappaB activation. J Biol Chem 274:22176-22183

44. Yang J, New L, Jiang Y, Han J, Su B 1998 Molecular cloning and characterization of a human protein kinase that specifically activates c-Jun N-terminal kinase. Gene 212:95-102

45. Kato Y, Kravchenko VV, Tapping RI, Han J, Ulevitch RJ, Lee JD 1997 BMK1/ERK5 regulates serum-induced early gene expression through transcription factor MEF2C. Embo J 16:7054-7066

Figure Legends

Fig. 1. MKK6 enhances ERE-activity in breast and endometrial carcinoma cells. MCF-7 (A) or Ishikawa (B) cells were cotransfected for 6 h with ERE-luciferase and empty vector (VEC) or CA-MKK6. Cells were then treated with DMSO or increasing concentrations of E2 (0.001-1.0 nM). The following day the cells were harvested for luciferase activity. Data is represented as % ERE activity normalized to vector transfected 1 nM E2-treated groups ± SE (n = 3). * $p < 0.05$, ** $p < 0.01$; significant differences from vehicle.

Fig. 2. RWJ67657 inhibits basal and exogenous MKK6-enhanced estrogen signaling. MCF-7 cells were transfected with ERE-luciferase and either empty vector (VEC) or CA-MKK6. 4 h later cells were treated overnight with vehicle (DMSO) or increasing concentrations of E2 (0.001-1.0 nM) in combination with vehicle (Veh) or 10 μM RWJ67657 (RWJ). The following day the cells were harvested for luciferase activity. Data is represented as % ERE activity normalized to vector transfected 1 nM E2-treated groups ± SE (n = 3). * $p < 0.05$, ** $p < 0.01$; significant differences from vehicle.

Fig. 3. MKK6 enhancement of ERE-activity in breast and endometrial carcinoma cells is ER dependent. MCF-7 (A) or Ishikawa (B) cells were cotransfected for 6 h with ERE-luciferase and empty vector (VEC) or CA-MKK6. Cells were then treated with DMSO or E2 (1 nM) alone or in combination with 100 nM ICI 182,780 (ICI) or 4-OH-tamoxifen (TAM). The following day the cells were harvested for luciferase activity. Data is represented as % ERE activity normalized to vector transfected 1 nM E2-treated groups ± SE (n = 3). * $p < 0.05$, ** $p < 0.01$; significant differences from vehicle.

Fig. 4. MKK6 enhances ERα and ERβ activity. HEK 293 cells were cotransfected for 6 h with ERE-luciferase and empty vector (VEC) or CA-MKK6 along with either hERα (A) or hERβ (B) expression plasmid. Cells were then treated overnight with DMSO or E2 (1 nM). The following day the cells were harvested for luciferase activity. Data is represented as % ERE activity normalized to vector transfected 1 nM E2-treated groups ± SE (n = 3). *** $p < 0.001$; significant differences from vehicle.

Fig. 5. RWJ67657 inhibits estrogen-stimulated colony formation of MCF-7 cells. MCF-7 cells were grown for 3 days in 5% DCC-FBS DMEM media and 1 x 10^3 cells were plated in 5% DCC-FBS DMEM dishes. The following day cells were treated with DMSO or E2 (1 nM) in combination with vehicle (DMSO) or 10 μM RWJ67657 (RWJ) for 24 h. The following day the media was changed to fresh 5% DCC-FBS DMEM media and colony formation was determined after 2 weeks. Data is represented as average number of colonies per treatment group from 3 wells ± SE (n = 3). ** $p < 0.01$, *** $p < 0.001$; significant differences from vehicle.

Fig. 6. MKK6 potentiates GRIP1. HEK 293 cells were cotransfected overnight with 25 ng of GAL4-GRIP1 full length along with a GAL4-luciferase reporter (50 ng) and 100 ng of empty expression vector or constitutively active MKK1, 5, 6, or 7. A CMV promoter drove all constitutive active MKK vectors. The following day luciferase activity was assayed. Results describe the fold induction over vehicle ± SE (n = 4). * $p < 0.05$; significant increases from control.

Fig. 7. DDT and its metabolites stimulate the p160 coactivator GRIP1 through the p38 MAPK. A, HEK 293 cells were cotransfected for 6 h with 25 ng empty GAL4 expression plasmid or GAL4-GRIP1 full length along with a GAL4-luciferase reporter

(50 ng) followed by overnight treatment as indicated in figure. B+C, HEK 293 cells were cotransfected overnight with 10 ng of GAL4-GRIP1 full length along with a GAL4-luciferase reporter (50 ng) and 0, 50, 100, or 150 ng of the indicated MAPK dominant-negative mutant (DN); either ERK2, JNK1, or p38α. A CMV promoter drove all dominant negative mutant expression vectors. Total DNA was equalized with an empty mammalian expression vector containing the same CMV promoter. The following day cells were treated overnight with DMSO (vehicle) (B) or 50 μM o,p'DDT (C). D, HEK 293 cells were cotransfected for 6 h with 25 ng empty GAL4 expression plasmid or GAL4-GRIP1 full length along with a GAL4-luciferase reporter (50 ng). After this period, the indicated concentration of kinase inhibitor was added, followed 30 min later by the addition of DMSO (vehicle) or o,p'DDT (50 μM). A-D, the day after treatments luciferase activity was assayed. A+D, results describe the fold induction over vehicle ± SE (n = 4). B+C, Each data point, presented as % of luciferase activity in the absence of MAPK mutants, represents the mean ± SE (n = 4-6). * $p < 0.05$, ** $p < 0.01$, *** $p < 0.001$; significant differences from vehicle or o,p'DDT treatment without inhibitor.

Fig. 8. Activated p38 phosphorylates GRIP1 *in vitro*. A, schematic of GST-fusion proteins used for *in vitro* kinase assays. B, GST fusion proteins were purified as described in "Materials and Methods" and standardized according to protein concentration. Purified activated p38 was then used to phosphorylate the GST-GRIP1 fragment in the presence of [γ-^{32}P]ATP at 30°C. Reactions were terminated by adding 2X sample loading buffer and running on SDS-PAGE gels. Gels were then dried and autoradiographed (right). Coomassie stained gels of GST proteins are on the left. Lower bands represent breakdown products of the GST fusion proteins as proven by the western

blot (data not shown). Proteins are identified by their size (kDa) with reference to molecular marker (lane 1). GST-MAPKAPK-2 was used as a positive control for p38 activity. Open arrow indicates phosphorylated GST-MAPKAPK-2 location. Closed arrows indicate phosphorylated GST-GRIP1 locations. Similar results were obtained in 3 independent experiments.

Fig. 9. Effect of p38 inhibitor (SB) and DDT on GAL4-GRIP1-NRID phosphorylation *in vivo*. A, COS-1 cells were transfected with expression vector GAL4-GRIP1-NRID followed by incubation with 0.27 mCi/ml [^{32}P]H_3PO_4 and treatment with vehicle (Veh), 6 μM SB203580 (SB), 25 μM o,p'DDT (DDT), or 6 μM SB + 25 μM DDT for 15 hours. Immunopurified GAL4-GRIP1-NRID was electrophoresed on a 10% SDS-polyacrylamide gel. A non-radioactive GAL4-GRIP1-NRID control was also included. The proteins were transferred to a nitrocellulose membrane and the membrane was exposed to X-AR film for autoradiography for 30 min (upper panel). Following autoradiography, the membrane was subjected to Western blotting with anti-GAL4-horseradish peroxidase antibody (lower panel). B, Normalized phosphorylation values for GAL4-GRIP1-NRID were calculated by dividing the value for the [^{32}P] signal by the value for the protein signal. Data were plotted as change in phosphorylation relative to vehicle treatment set at a value of 1 ± SE (n = 3). * $p < 0.05$, significant changes from vehicle; †$p < 0.05$, significant changes from DDT alone treated.

Fig. 10. Effect of constitutive active MKK6 or o,p'DDT on the transcriptional activity of different GRIP1 domains/mutants. A, Schematic of GAL4-fusion protein constructs used for mammalian one-hybrid assays. B, HEK 293 cells were cotransfected for 6 h with 25 ng of GAL4 empty expression vector or different GAL4-GRIP1 full length or mutant

vectors as indicated in the figures along with a GAL4-luciferase reporter (50 ng). Hashed bars represent cells that were also transfected overnight with 100 ng of empty expression vector or constitutive active MKK6 (CA-MKK6). Black bars represent cells that were then treated overnight with DMSO (vehicle) or o,p'DDT (50 μM). The following day luciferase activity was assayed. Results describe the fold stimulation over vehicle-transfected cells (hashed bars) or vehicle treated cells (black bars) ± SE (n = 4). * $p < 0.05$, ** $p < 0.01$, *** $p < 0.001$; significant changes from control.

Fig. 11. Effect of p38 inhibitor (SB) and DDT on GAL4-GRIP1-NRID S736A phosphorylation *in vivo*. A, COS-1 cells were transfected with expression vector GAL4-GRIP1-NRID or GAL4-GRIP1-NRID-S736A followed by incubation with 0.27 mCi/ml $[^{32}P]H_3PO_4$ and treatment with vehicle (Veh), 6 μM SB203580 (SB), 25 μM o,p'DDT (DDT), or 6 μM SB + 25 μM DDT for 15 hours. Immunopurified GAL4-GRIP1-NRID or GAL4-GRIP1-NRID-S736A was electrophoresed on a 10% SDS-polyacrylamide gel. GAL4-GRIP1-NRID protein immunopurified with normal mouse IgG was also run as a negative control. A non-radioactive GAL4-GRIP1-NRID control was also included. The proteins were transferred to a nitrocellulose membrane and the membrane was exposed to X-AR film for autoradiography for 30 min (upper panel). Following autoradiography, the membrane was subjected to Western blotting with anti-GAL4-horseradish peroxidase antibody (lower panel). B, Normalized phosphorylation values for GAL4-GRIP1-NRID constructs were calculated by dividing the value for the $[^{32}P]$ signal by the value for the protein signal. Data were plotted as change in phosphorylation relative to NRID(wt)-vehicle treatment set at a value of 1 ± SE (n = 3). * $p < 0.05$, significant changes from NRID(wt)-vehicle treatment.

Fig. 12. The GRIP1 mutation S736A blocks MKK6's ability to potentiate ER-mediated transcription. MCF-7 cells stably transfected with either empty expression vector (MCF-7-Vec; white bars) or CA-MKK6 (MCF-7-MKK6; grey bars) were cotransfected for 5 h with 300 ng pERE-Luc and 200 ng of pSG5, pSG5-GRIP1, or pSG5-GRIP1 S736A. Cells were then treated overnight with vehicle (DMSO) or 100 pM E2. The following day luciferase activity was assayed. Results are described as mean activity normalized to E2 induction (set at 100%) of MCF-7-Vec cells transfected with empty pSG5 ± SE (n = 3).

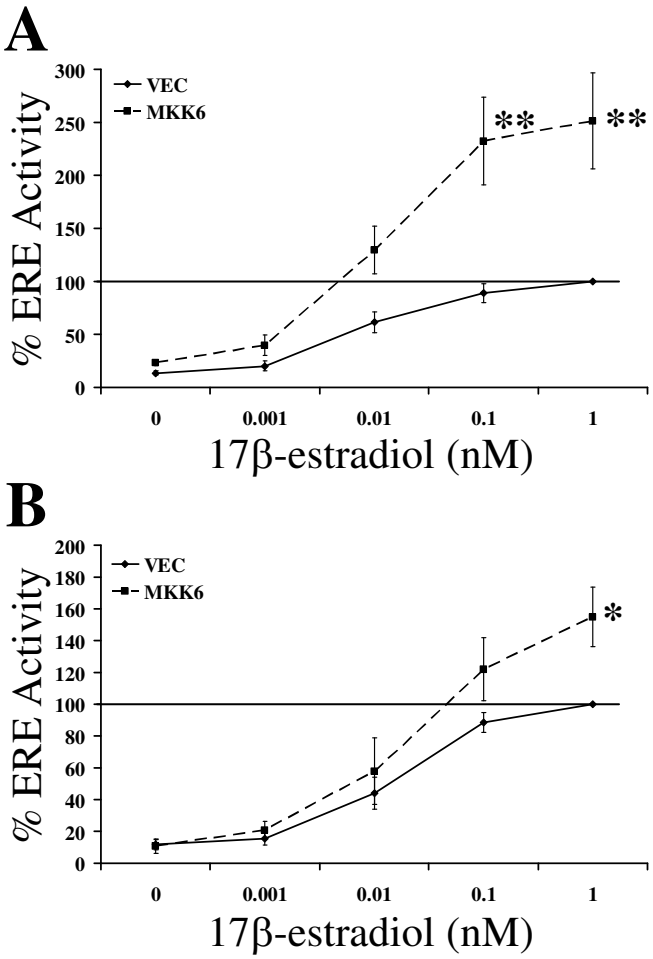
A
300
250
200
150
100
50
0
VEC
MKK6
**
**
% ERE Activity
0
0.001
0.01
0.1
1
17β-estradiol (nM)
B
200
180
160
140
120
100
80
60
40
20
0
VEC
MKK6
*
% ERE Activity
0
0.001
0.01
0.1
1
17β-estradiol (nM)

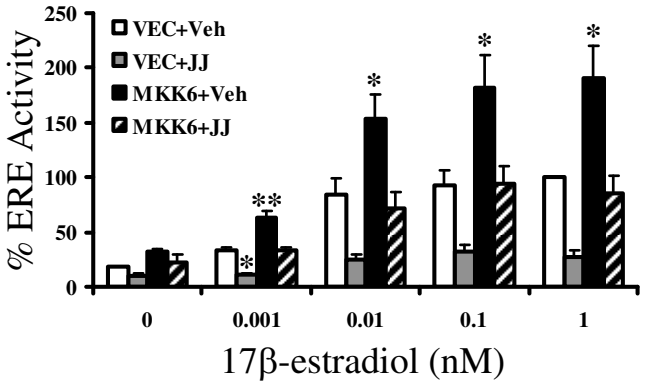
250
200
150
100
50
0
% ERE Activity
VEC+Veh
VEC+JJ
MKK6+Veh
MKK6+JJ
**
*
*
*
0
0.001
0.01
0.1
1
17β-estradiol (nM)

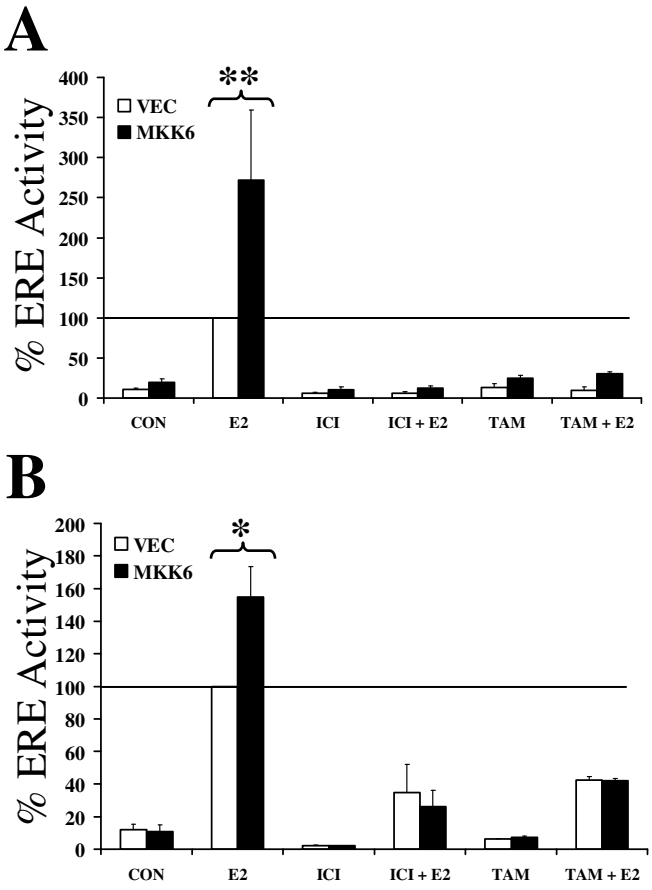
A
% ERE Activity
400
350
300
250
200
150
100
50
0
VEC
MKK6
**
CON
E2
ICI
ICI + E2
TAM
TAM + E2
B
% ERE Activity
200
180
160
140
120
100
80
60
40
20
0
VEC
MKK6
*
CON
E2
ICI
ICI + E2
TAM
TAM + E2

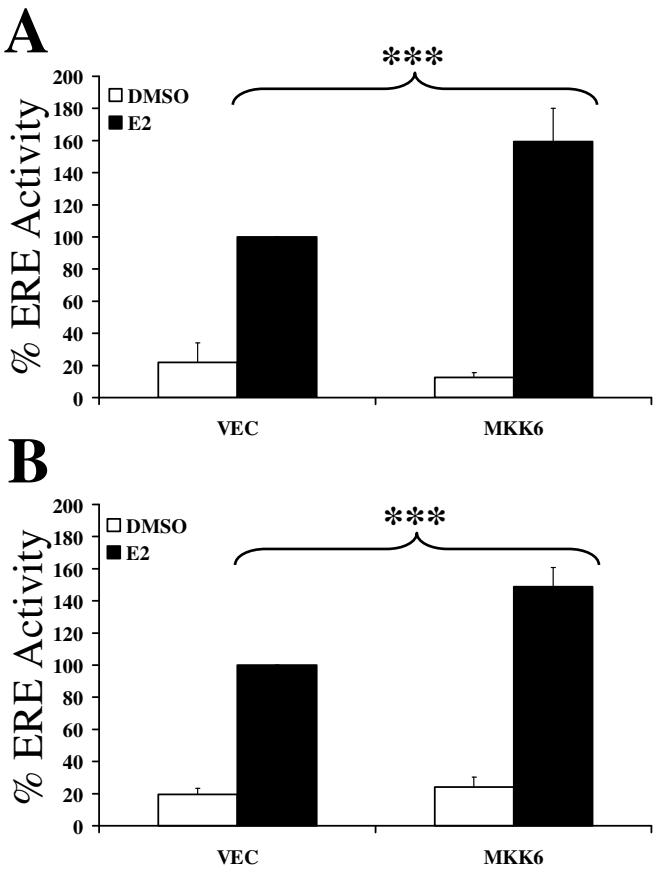
A
***
DMSO
E2
% ERE Activity
200
180
160
140
120
100
80
60
40
20
0
VEC
MKK6
B
***
DMSO
E2
% ERE Activity
200
180
160
140
120
100
80
60
40
20
0
VEC
MKK6

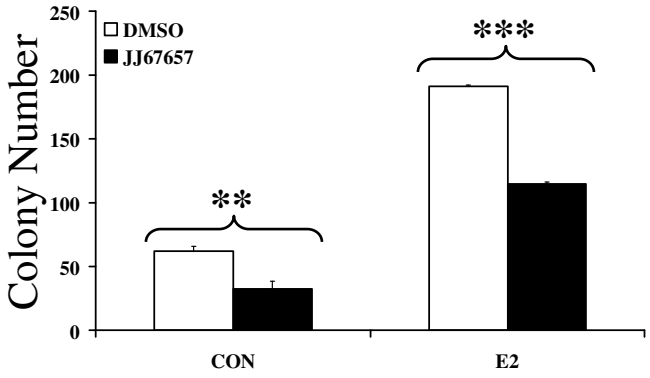
Colony Number
250
200
150
100
50
0
DMSO
JJ67657
**
***
CON
E2

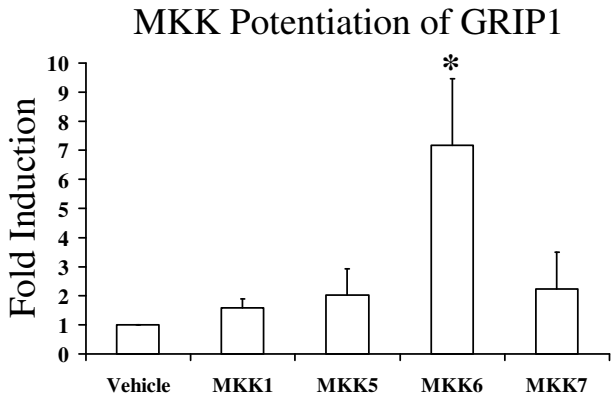
MKK Potentiation of GRIP1
Fold Induction
10
9
8
7
6
5
4
3
2
1
0
*
Vehicle
MKK1
MKK5
MKK6
MKK7

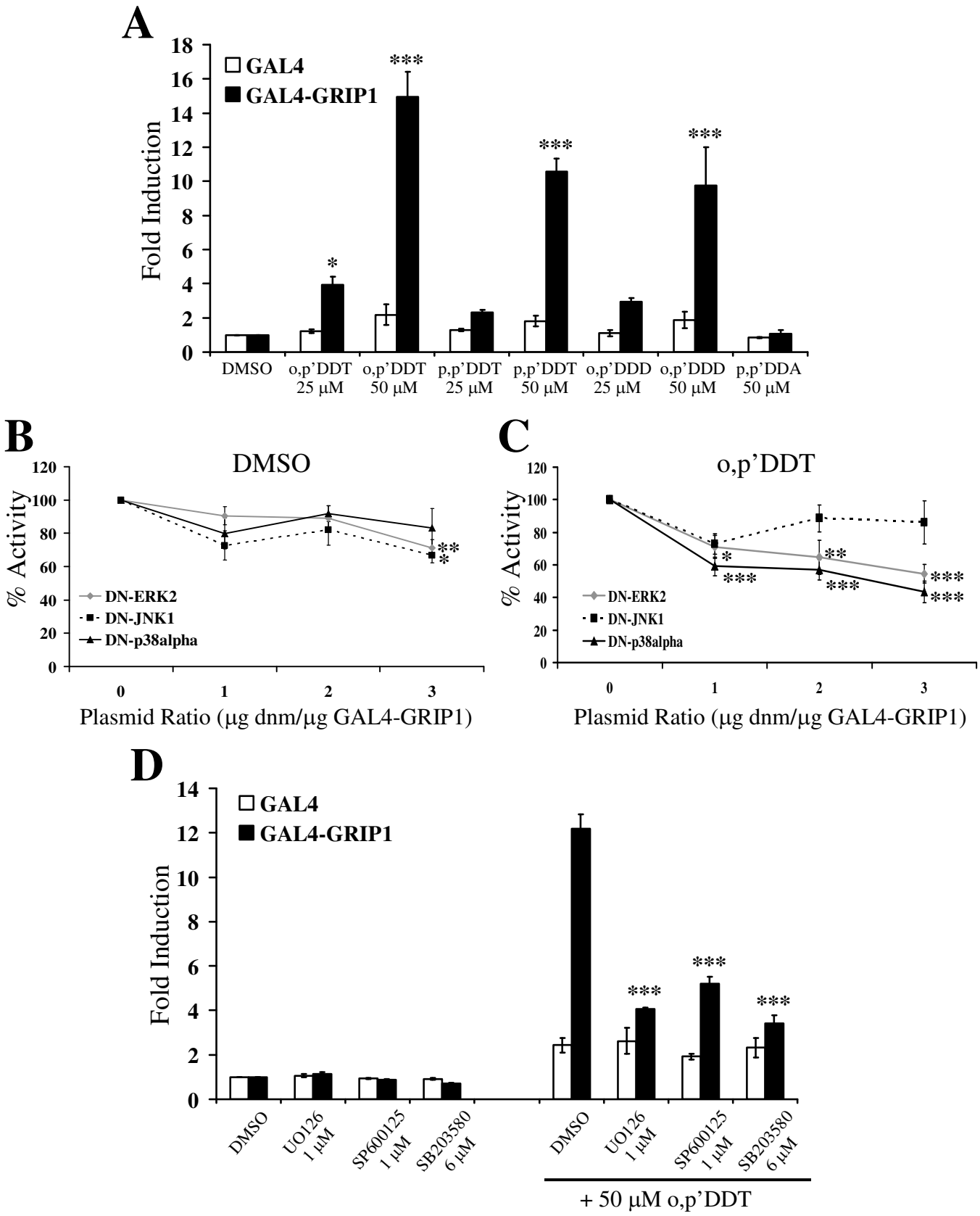
A
GAL4
GAL4-GRIP1
Fold Induction
DMSO
o,p'DDT 25 μM
o,p'DDT 50 μM
p,p'DDT 25 μM
p,p'DDT 50 μM
o,p'DDD 25 μM
o,p'DDD 50 μM
p,p'DDA 50 μM
B
DMSO
% Activity
DN-ERK2
DN-JNK1
DN-p38alpha
Plasmid Ratio (μg dnm/μg GAL4-GRIP1)
C
o,p'DDT
% Activity
DN-ERK2
DN-JNK1
DN-p38alpha
Plasmid Ratio (μg dnm/μg GAL4-GRIP1)
D
GAL4
GAL4-GRIP1
Fold Induction
DMSO
UO126 1 μM
SP600125 1 μM
SB203580 6 μM
DMSO
UO126 1 μM
SP600125 1 μM
SB203580 6 μM
+ 50 μM o,p'DDT

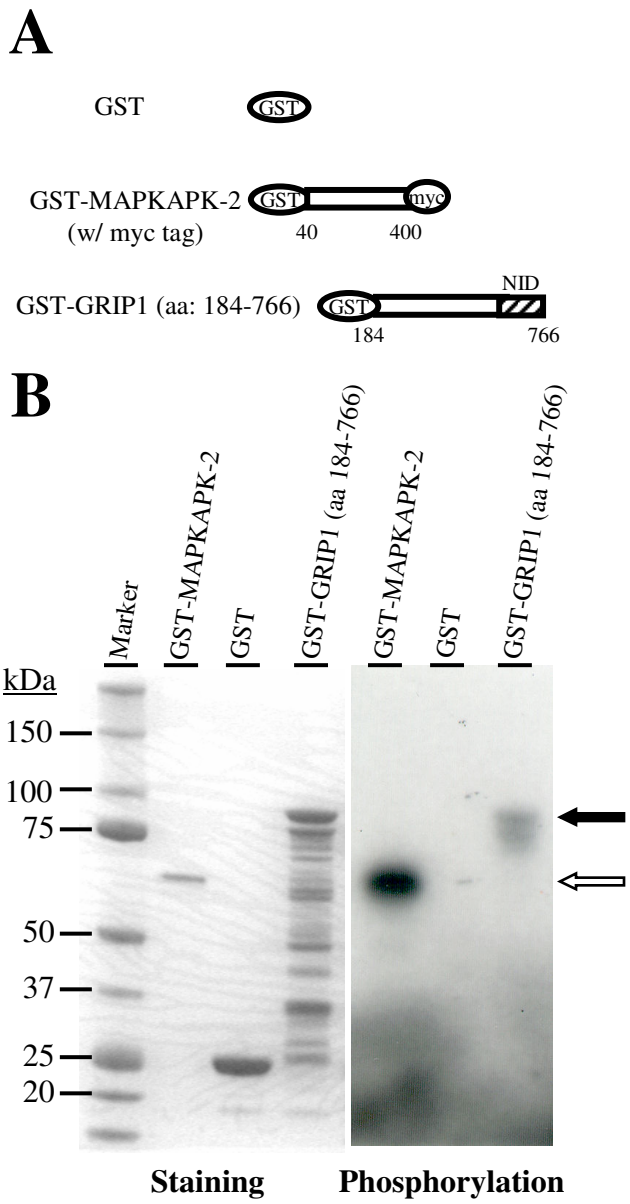
A
GST
GST
GST-MAPKAPK-2
(w/ myc tag)
GST
myc
40
400
GST-GRIP1 (aa: 184-766)
NID
GST
184
766
B
Marker
GST-MAPKAPK-2
GST
GST-GRIP1 (aa 184-766)
GST-MAPKAPK-2
GST
GST-GRIP1 (aa 184-766)
kDa
150
100
75
50
37
25
20
Staining
Phosphorylation

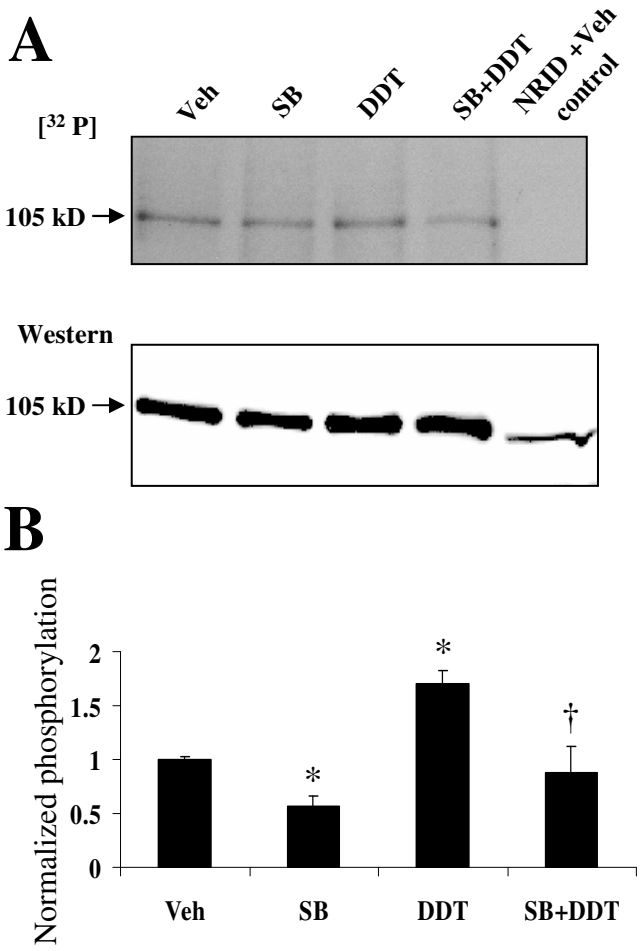
A
Veh
SB
DDT
SB+DDT
NRID +Veh control
[32 P]
105 kD
Western
105 kD
B
Normalized phosphorylation
2
1.5
1
0.5
0
*
*
†
Veh
SB
DDT
SB+DDT

A

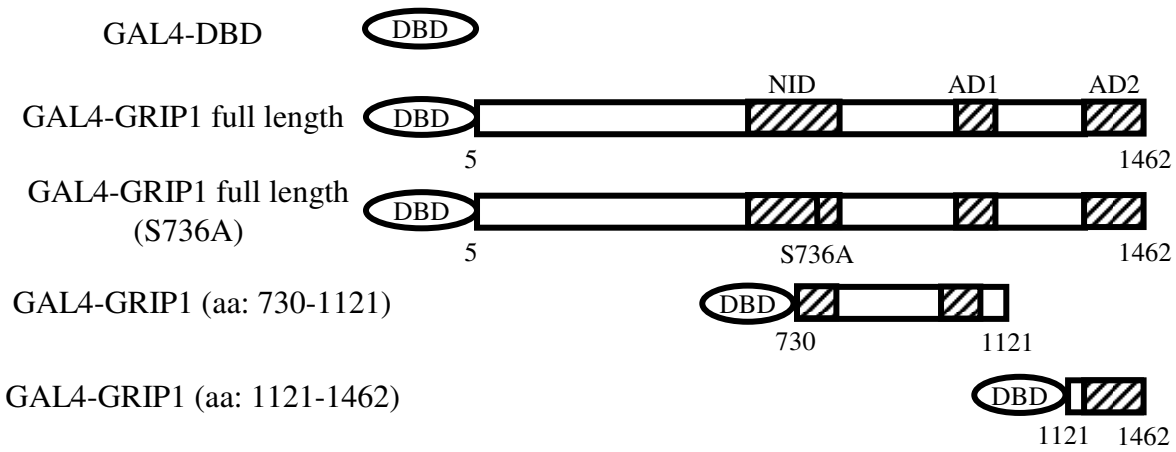
GAL4-DBD
DBD
GAL4-GRIP1 full length
NID
AD1
AD2
5
1462
GAL4-GRIP1 full length (S736A)
S736A
GAL4-GRIP1 (aa: 730-1121)
730
1121
GAL4-GRIP1 (aa: 1121-1462)
1121
1462

B

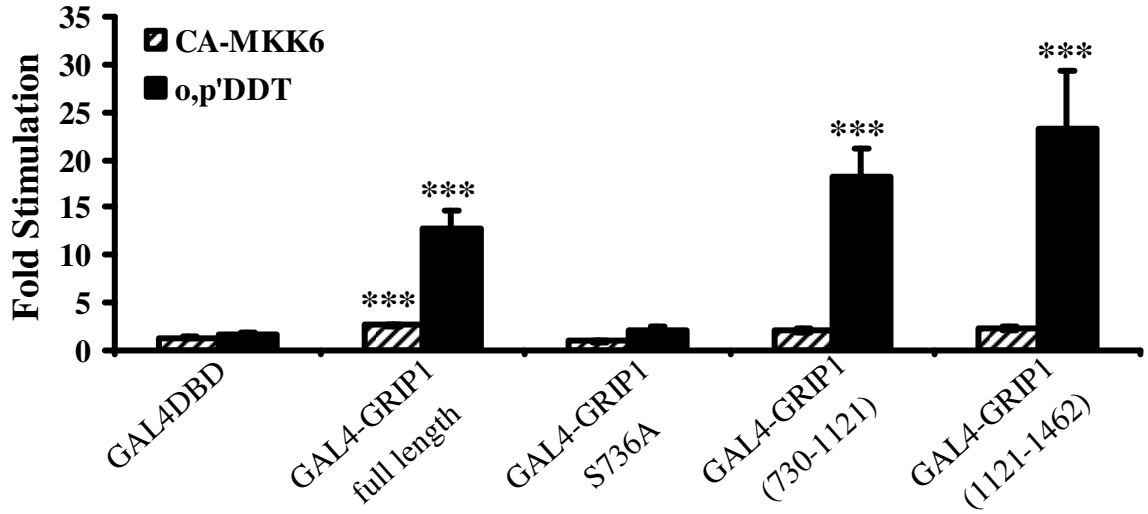
Fold Stimulation
CA-MKK6
o,p'DDT
***
GAL4DBD
GAL4-GRIP1 full length
GAL4-GRIP1 S736A
GAL4-GRIP1 (730-1121)
GAL4-GRIP1 (1121-1462)

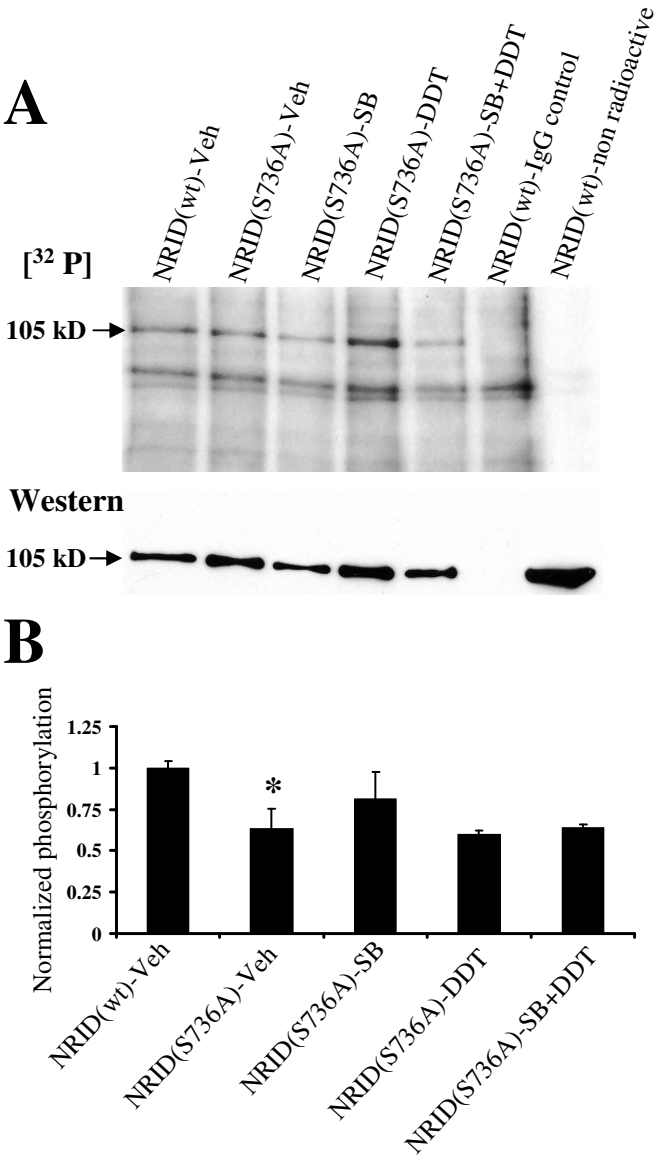
A
NRID(wt)-Veh
NRID(S736A)-Veh
NRID(S736A)-SB
NRID(S736A)-DDT
NRID(S736A)-SB+DDT
NRID(wt)-IgG control
NRID(wt)-non radioactive
[32 P]
105 kD
Western
105 kD
B
Normalized phosphorylation
1.25
1
0.75
0.5
0.25
0
*
NRID(wt)-Veh
NRID(S736A)-Veh
NRID(S736A)-SB
NRID(S736A)-DDT
NRID(S736A)-SB+DDT

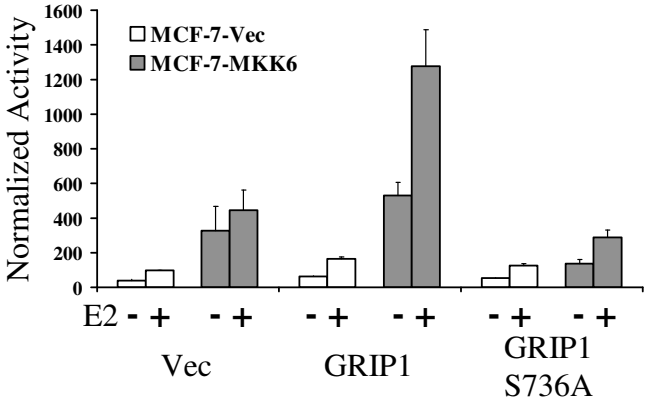
Normalized Activity
1600
1400
1200
1000
800
600
400
200
0
MCF-7-Vec
MCF-7-MKK6
E2 - + - + - + - + - + - +
Vec
GRIP1
GRIP1
S736A